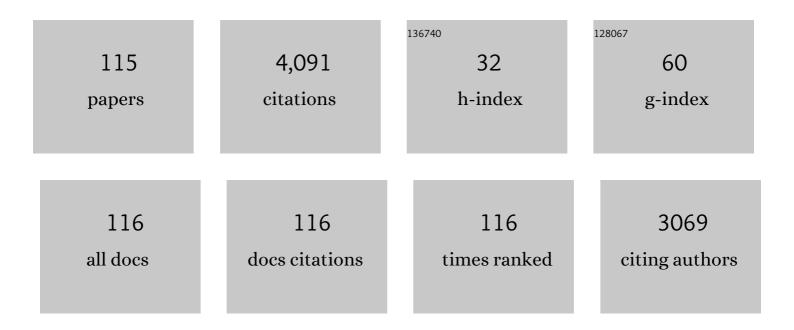
Shaofeng Wang

List of Publications by Year in descending order

Source: https://exaly.com/author-pdf/951958/publications.pdf Version: 2024-02-01



#	Article	IF	CITATIONS
1	Human Exposure To Methylmercury through Rice Intake in Mercury Mining Areas, Guizhou Province, China. Environmental Science & Technology, 2008, 42, 326-332.	4.6	394
2	Methylmercury Accumulation in Rice (Oryza sativa L.) Grown at Abandoned Mercury Mines in Guizhou, China. Journal of Agricultural and Food Chemistry, 2008, 56, 2465-2468.	2.4	226
3	Mercury and methylmercury in riparian soil, sediments, mine-waste calcines, and moss from abandoned Hg mines in east Guizhou province, southwestern China. Applied Geochemistry, 2005, 20, 627-638.	1.4	212
4	A review of studies on atmospheric mercury in China. Science of the Total Environment, 2012, 421-422, 73-81.	3.9	188
5	Environmental contamination of mercury from Hg-mining areas in Wuchuan, northeastern Guizhou, China. Environmental Pollution, 2006, 142, 549-558.	3.7	162
6	Fractionation of heavy metals in shallow marine sediments from Jinzhou Bay, China. Journal of Environmental Sciences, 2010, 22, 23-31.	3.2	127
7	Total gaseous mercury concentrations in ambient air in the eastern slope of Mt. Congga, South-Eastern fringe of the Tibetan plateau, China. Atmospheric Environment, 2008, 42, 970-979.	1.9	126
8	Temporal variation of total gaseous mercury in the air of Guiyang, China. Journal of Geophysical Research, 2004, 109, n/a-n/a.	3.3	109
9	Total mercury and monomethylmercury in water, sediments, and hydrophytes from the rivers, estuary, and bay along the Bohai Sea coast, northeastern China. Applied Geochemistry, 2009, 24, 1702-1711.	1.4	93
10	Mercury exposure in the population from Wuchuan mercury mining area, Guizhou, China. Science of the Total Environment, 2008, 395, 72-79.	3.9	92
11	Characteristics of mercury exchange flux between soil and air in the heavily air-polluted area, eastern Guizhou, China. Atmospheric Environment, 2007, 41, 5584-5594.	1.9	90
12	Total particulate and reactive gaseous mercury in ambient air on the eastern slope of the Mt. Gongga area, China. Applied Geochemistry, 2008, 23, 408-418.	1.4	82
13	Giving waterbodies the treatment they need: A critical review of the application of constructed floating wetlands. Journal of Environmental Management, 2019, 238, 484-498.	3.8	82
14	Incorporation of arsenic into gypsum: Relevant to arsenic removal and immobilization process in hydrometallurgical industry. Journal of Hazardous Materials, 2015, 300, 272-280.	6.5	80
15	Total gaseous mercury emissions from soil in Guiyang, Guizhou, China. Journal of Geophysical Research, 2005, 110, n/a-n/a.	3.3	79
16	Seasonal variation of gaseous mercury exchange rate between air and water surface over Baihua reservoir, Guizhou, China. Atmospheric Environment, 2004, 38, 4721-4732.	1.9	78
17	Mercury distribution and speciation in water and fish from abandoned Hg mines in Wanshan, Guizhou province, China. Science of the Total Environment, 2009, 407, 5162-5168.	3.9	76
18	Mercury contaminations from historic mining to water, soil and vegetation in Lanmuchang, Guizhou, southwestern China. Science of the Total Environment, 2006, 368, 56-68.	3.9	72

#	Article	IF	CITATIONS
19	Mercury pollution in Wuchuan mercury mining area, Guizhou, Southwestern China: The impacts from large scale and artisanal mercury mining. Environment International, 2012, 42, 59-66.	4.8	71
20	Temporal and spatial distributions of total gaseous mercury concentrations in ambient air in a mountainous area in southwestern China: Implications for industrial and domestic mercury emissions in remote areas in China. Science of the Total Environment, 2009, 407, 2306-2314.	3.9	67
21	Transformation of arsenic in offshore sediment under the impact of anaerobic microbial activities. Water Research, 2011, 45, 6781-6788.	5.3	67
22	Mercury concentrations and air/soil fluxes in Wuchuan mercury mining district, Guizhou province, China. Atmospheric Environment, 2007, 41, 5984-5993.	1.9	56
23	Exchange fluxes of Hg between surfaces and atmosphere in the eastern flank of Mount Gongga, Sichuan province, southwestern China. Journal of Geophysical Research, 2008, 113, .	3.3	52
24	Speciation change and redistribution of arsenic in soil under anaerobic microbial activities. Journal of Hazardous Materials, 2016, 301, 538-546.	6.5	51
25	The variations of mercury in sediment profiles from a historically mercury-contaminated reservoir, Guizhou province, China. Science of the Total Environment, 2008, 407, 497-506.	3.9	48
26	Arsenic retention and remobilization in muddy sediments with high iron and sulfur contents from a heavily contaminated estuary in China. Chemical Geology, 2012, 314-317, 57-65.	1.4	48
27	Atmospheric mercury emission from artisanal mercury mining in Guizhou Province, Southwestern China. Atmospheric Environment, 2009, 43, 2247-2251.	1.9	47
28	Arsenic redistribution and transformation during Fe(II)-catalyzed recrystallization of As-adsorbed ferrihydrite under anaerobic conditions. Chemical Geology, 2019, 525, 380-389.	1.4	46
29	Simultaneous removal and oxidation of arsenic from water by δ-MnO2 modified activated carbon. Journal of Environmental Sciences, 2020, 94, 147-160.	3.2	43
30	The distribution of total mercury and methyl mercury in a shallow hypereutrophic lake (Lake Taihu) in two seasons. Applied Geochemistry, 2012, 27, 343-351.	1.4	39
31	The Transformation of Two-Line Ferrihydrite into Crystalline Products: Effect of pH and Media (Sulfate versus Nitrate). ACS Earth and Space Chemistry, 2018, 2, 577-587.	1.2	38
32	Effect of hydroquinone-induced iron reduction on the stability of scorodite and arsenic mobilization. Hydrometallurgy, 2016, 164, 228-237.	1.8	33
33	Simultaneous oxidation and removal of Sb(III) from water by using synthesized CTAB/MnFe2O4/MnO2 composite. Chemosphere, 2020, 245, 125601.	4.2	32
34	Bioaccumulation and trophic transfer of mercury in a food web from a large, shallow, hypereutrophic lake (Lake Taihu) in China. Environmental Science and Pollution Research, 2012, 19, 2820-2831.	2.7	31
35	Arsenic associated with gypsum produced from Fe(III)-As(V) coprecipitation: Implications for the stability of industrial As-bearing waste. Journal of Hazardous Materials, 2018, 360, 311-318.	6.5	31
36	Effects of nutrient and sulfate additions on As mobility in contaminated soils: A laboratory column study. Chemosphere, 2015, 119, 902-909.	4.2	29

#	Article	IF	CITATIONS
37	Comparison of mercury speciation and distribution in the water column and sediments between the algal type zone and the macrophytic type zone in a hypereutrophic lake (Dianchi Lake) in Southwestern China. Science of the Total Environment, 2012, 417-418, 204-213.	3.9	28
38	Lanthanum hydroxide: a highly efficient and selective adsorbent for arsenate removal from aqueous solution. Environmental Science and Pollution Research, 2020, 27, 42868-42880.	2.7	28
39	The long-term stability of calcium arsenates: Implications for phase transformation and arsenic mobilization. Journal of Environmental Sciences, 2019, 84, 29-41.	3.2	27
40	Sequestration of Selenite and Selenate in Gypsum (CaSO ₄ ·2H ₂ O): Insights from the Single-Crystal Electron Paramagnetic Resonance Spectroscopy and Synchrotron X-ray Absorption Spectroscopy Study. Environmental Science & Technology, 2020, 54, 3169-3180.	4.6	27
41	Spectroscopic and DFT study on the species and local structure of arsenate incorporated in gypsum lattice. Chemical Geology, 2017, 460, 46-53.	1.4	26
42	Adsorption of monothioarsenate on amorphous aluminum hydroxide under anaerobic conditions. Chemical Geology, 2015, 407-408, 46-53.	1.4	25
43	Arsenic release and speciation during the oxidative dissolution of arsenopyrite by O2 in the absence and presence of EDTA. Journal of Hazardous Materials, 2018, 346, 184-190.	6.5	25
44	The long-term stability of FeIII-AsV coprecipitates at pH 4 and 7: Mechanisms controlling the arsenic behavior. Journal of Hazardous Materials, 2019, 374, 276-286.	6.5	25
45	A novel method for preparing an As(V) solution for scorodite synthesis from an arsenic sulphide residue in a Pb refinery. Hydrometallurgy, 2019, 183, 1-8.	1.8	25
46	New Insight into the Local Structure of Hydrous Ferric Arsenate Using Full-Potential Multiple Scattering Analysis, Density Functional Theory Calculations, and Vibrational Spectroscopy. Environmental Science & Technology, 2016, 50, 12114-12121.	4.6	24
47	Bacterial reduction and release of adsorbed arsenate on Fe(III)-, Al- and coprecipitated Fe(III)/Al-hydroxides. Journal of Environmental Sciences, 2012, 24, 440-448.	3.2	23
48	Rapid abiotic As removal from As-rich acid mine drainage: Effect of pH, Fe/As molar ratio, oxygen, temperature, initial As concentration and neutralization reagent. Chemical Engineering Journal, 2019, 378, 122156.	6.6	23
49	The fate of co-existent cadmium and arsenic during Fe(II)-induced transformation of As(V)/Cd(II)-bearing ferrihydrite. Chemosphere, 2022, 301, 134665.	4.2	23
50	Spatial and seasonal variations in soil and river water mercury in a boreal forest, Changbai Mountain, Northeastern China. Geoderma, 2013, 206, 123-132.	2.3	21
51	Effect of sulfide on As(III) and As(V) sequestration by ferrihydrite. Chemosphere, 2017, 185, 321-328.	4.2	21
52	Photocatalytic Activity of Fe and Ce Coâ€doped Mesoporous TiO ₂ Catalyst under UV and Visible Light. Journal of the Chinese Chemical Society, 2012, 59, 614-620.	0.8	20
53	The stability of Fe(III)-As(V) co-precipitate in the presence of ascorbic acid: Effect of pH and Fe/As molar ratio. Chemosphere, 2019, 218, 670-679.	4.2	20
54	Detoxification and reclamation of hydrometallurgical arsenic- and trace metals-bearing gypsum via hydrothermal recrystallization in acid solution. Chemosphere, 2020, 250, 126290.	4.2	20

#	Article	IF	CITATIONS
55	Total gaseous mercury exchange between water and air during cloudy weather conditions over Hongfeng Reservoir, Guizhou, China. Journal of Geophysical Research, 2008, 113, .	3.3	19
56	Alternative Method for the Treatment of Hydrometallurgical Arsenic–Calcium Residues: The Immobilization of Arsenic as Scorodite. ACS Omega, 2020, 5, 12979-12988.	1.6	19
57	Occurrence state of co-existing arsenate and nickel ions at the ferrihydrite-water interface: Mechanisms of surface complexation and surface precipitation via ATR-IR spectroscopy. Chemosphere, 2018, 206, 33-42.	4.2	17
58	The adsorption behavior of thioarsenite on magnetite and ferrous sulfide. Chemical Geology, 2018, 492, 1-11.	1.4	17
59	Molecular speciation of phosphorus in phosphogypsum waste by solid-state nuclear magnetic resonance spectroscopy. Science of the Total Environment, 2019, 696, 133958.	3.9	17
60	Stabilization and transformation of selenium during the Fe(II)-induced transformation of Se(IV)-adsorbed ferrihydrite under anaerobic conditions. Journal of Hazardous Materials, 2020, 384, 121365.	6.5	16
61	The adsorption of As(V) on poorly crystalline Fe oxyhydroxides, revisited: Effect of the reaction media and the drying treatment. Journal of Hazardous Materials, 2021, 416, 125863.	6.5	15
62	A qualitative and quantitative investigation of partitioning and local structure of arsenate in barite lattice during coprecipitation of barium, sulfate, and arsenate. American Mineralogist, 2017, 102, 2512-2520.	0.9	14
63	Long-term stability of the Fe(III)–As(V) coprecipitates: Effects of neutralization mode and the addition of Fe(II) on arsenic retention. Chemosphere, 2019, 237, 124503.	4.2	14
64	Co-adsorption of arsenite and arsenate on mixed-valence Fe(II,III) (hydr)oxides under reducing conditions. Applied Geochemistry, 2018, 98, 418-425.	1.4	13
65	Mechanism of Gd3+ uptake in gypsum (CaSO4·2H2O): Implications for EPR dating, REE recovery and REE behavior. Geochimica Et Cosmochimica Acta, 2019, 258, 63-78.	1.6	13
66	Incorporation of trace metals Cu, Zn, and Cd into gypsum: Implication on their mobility and fate in natural and anthropogenic environments. Chemical Geology, 2020, 541, 119574.	1.4	13
67	Arsenic removal from hydrometallurgical waste sulfuric acid via scorodite formation using siderite (FeCO3). Chemical Engineering Journal, 2021, 424, 130552.	6.6	13
68	Characterization of Fe5(AsO3)3Cl2(OH)4·5H2O, a new ferric arsenite hydroxychloride precipitated from FeCl3–As2O3–HCl solutions relevant to arsenic immobilization. Journal of Environmental Sciences, 2020, 90, 205-215.	3.2	12
69	Fate of arsenic during up to 4.5Âyears of aging of Felll-AsV coprecipitates at acidic pH: Effect of reaction media (Nitrate vs. Sulfate), Fe/As molar ratio, and pH. Chemical Engineering Journal, 2020, 388, 124239.	6.6	12
70	Oxidation and incorporation of adsorbed antimonite during iron(II)-catalyzed recrystallization of ferrihydrite. Science of the Total Environment, 2021, 778, 146424.	3.9	11
71	Degradation of organic matter in the sediments of Hongfeng Reservoir. Science Bulletin, 2005, 50, 2377-2380.	1.7	10
72	Adsorption Behavior and Removal Mechanism of Arsenic from Water by Fe(III)-Modified 13X Molecular Sieves. Water, Air, and Soil Pollution, 2016, 227, 1.	1.1	10

#	Article	IF	CITATIONS
73	The effect of microbial sulfidogenesis on the stability of As–Fe coprecipitate with low Fe/As molar ratio under anaerobic conditions. Environmental Science and Pollution Research, 2016, 23, 7267-7277.	2.7	10
74	Adsorption and transformation of thioarsenite at hematite/water interface under anaerobic condition in the presence of sulfide. Chemosphere, 2019, 222, 422-430.	4.2	10
75	Stabilization of Scorodite by Aluminum Silicate Microencapsulation. Journal of Environmental Engineering, ASCE, 2019, 145, .	0.7	10
76	A combined abiotic oxidation-precipitation process for rapid As removal from high-As(III)-Mn(II) acid mine drainage and low As-leaching solid products. Journal of Hazardous Materials, 2021, 401, 123360.	6.5	10
77	Physical properties of nano-titania hollow fibers and their photocatalytic activity in the decomposition of phenol. Russian Journal of Physical Chemistry A, 2013, 87, 69-73.	0.1	9
78	An alternative method for the treatment of metallurgical arsenic-alkali residue and recovery of high-purity sodium bicarbonate. Hydrometallurgy, 2021, 202, 105590.	1.8	9
79	Phase transformation of hydrous ferric arsenate in the presence of Fe(II) under anaerobic conditions: Implications for arsenic mobility and fate in natural and anthropogenic environments. Chemical Geology, 2021, 578, 120321.	1.4	9
80	A novel method for in situ stabilization of calcium arsenic residues via yukonite formation. Science of the Total Environment, 2022, 819, 153090.	3.9	9
81	Effect of hydroquinone-induced iron reduction on the stability of Fe(III)-As(V) Co-precipitate and arsenic mobilization. Applied Geochemistry, 2018, 97, 1-10.	1.4	8
82	A new and improved synthesis method for the formation of ZnFe-CO3 and ZnFe-SO4 Hydrotalcites free from impurities. Applied Clay Science, 2019, 181, 105215.	2.6	8
83	Fate of adsorbed arsenic during early stage sulfidization of nano-ferrihydrite. Environmental Science: Nano, 2019, 6, 2228-2240.	2.2	8
84	Assessment of metal contamination in the Hun River, China, and evaluation of the fish Zacco platypus and the snail Radix swinhoei as potential biomonitors. Environmental Science and Pollution Research, 2017, 24, 6512-6522.	2.7	7
85	Accurate determination of the As(<scp>v</scp>) coordination environment at the surface of ferrihydrite using synchrotron extended X-ray absorption fine structure spectroscopy and <i>ab initio</i> Debye–Waller factors. Environmental Science: Nano, 2019, 6, 2441-2451.	2.2	7
86	Partitioning and transformation behavior of arsenic during Fe(III)-As(III)-As(V)-SO42â^' coprecipitation and subsequent aging process in acidic solutions: Implication for arsenic mobility and fixation. Science of the Total Environment, 2021, 799, 149474.	3.9	7
87	Effect of iron reduction by enolic hydroxyl groups on the stability of scorodite in hydrometallurgical industries and arsenic mobilization. Environmental Science and Pollution Research, 2017, 24, 26534-26544.	2.7	6
88	Insight into the effect of SO42â^' on the precipitation and solubility of ferric arsenate in acidic solutions: Implication for arsenic mobility and fate. Chemical Geology, 2022, 602, 120900.	1.4	6
89	Photocatalytic degradation of methylene blue by visible-light-driven yttrium-doped mesoporous titania coated magnetite photocatalyst. Desalination and Water Treatment, 2013, 51, 7101-7108.	1.0	5
90	Effects of sediment composition on cadmium bioaccumulation in the clam <i>Meretrix meretrix</i> Linnaeus. Environmental Toxicology and Chemistry, 2013, 32, 841-847.	2.2	5

#	Article	IF	CITATIONS
91	The Effects of Solution Concentration, Drying, Aging Time, and Mixture of Goethite with As(V)-Fe(OH)3 on the Chemical Extraction of Arsenate Associated with Iron (Hydr)oxides. Environmental Engineering Science, 2017, 34, 443-452.	0.8	5
92	Surface Sorption Site and Complexation Structure of Ca2+ at the Goethite–Water Interface: A Molecular Dynamics Simulation and Quantitative XANES Analysis. Bulletin of Environmental Contamination and Toxicology, 2019, 103, 64-68.	1.3	5
93	Further insights into the Fe(<scp>ii</scp>) reduction of 2-line ferrihydrite: a semi <i>in situ</i> and <i>in situ</i> TEM study. Nanoscale Advances, 2020, 2, 4938-4950.	2.2	5
94	The effect of iron reduction on the long-term stability of scorodite in the presence of enolic hydroxyl groups and mineral transformation. Applied Geochemistry, 2020, 122, 104730.	1.4	5
95	The effects of pH, neutralizing reagent and co-ions on Mo(VI) removal and speciation in Fe(III)–Mo(VI) coprecipitation process. Applied Geochemistry, 2021, 134, 105091.	1.4	5
96	Biotic and Abiotic Controls on Dinitrogen Production in Coastal Sediments. Global Biogeochemical Cycles, 2021, 35, e2021GB007069.	1.9	5
97	Effects of pore size and dissolved organic matters on diffusion of arsenate in aqueous solution. Journal of Environmental Sciences, 2017, 52, 190-196.	3.2	4
98	Removal of As(V) and As(III) species from wastewater by adsorption on coal fly ash. , 0, 151, 242-250.		4
99	Effect of co-existent Al(III) in As-rich Acid Mine Drainage (AMD) on As removal during Fe(II) and As(III) abiotic oxidation process. Journal of Water Process Engineering, 2021, 44, 102395.	2.6	4
100	Abiotic anoxic reduction of AsO4 adsorbed Mg(II)–Al(III)/Fe(III)–CO3/SO4 Layered Double Hydroxides: Implications of As release and phase transformations. Applied Geochemistry, 2020, 122, 104765.	1.4	3
101	Application of the RUSLE for Determining Riverine Heavy Metal Flux in the Upper Pearl River Basin, China. Bulletin of Environmental Contamination and Toxicology, 2021, 106, 24-32.	1.3	3
102	Molecular structures of dissolved and colloidal AsV–FeIII complexes and their roles in the mobilization of AsV under strongly acidic conditions. Journal of Hazardous Materials, 2022, 430, 128266.	6.5	3
103	Arsenite oxidation and (thio)arsenates formation in arsenite- and sulfide-containing solution under air atmosphere. Applied Geochemistry, 2022, 142, 105344.	1.4	3
104	Preparation and characterization of sulfur-modified mesoporous titania photocatalyst. Russian Journal of Physical Chemistry A, 2013, 87, 1300-1305.	0.1	2
105	Molecular Structure of Molybdate Adsorption on Goethite at pH 5–8: A Combined DFT + U, EXAFS, and Ab Initio XANES Study. Journal of Physical Chemistry C, 2021, 125, 22052-22063.	1.5	2
106	Observation of surface precipitation of ferric molybdate on ferrihydrite: Implication for the mobility and fate of molybdate in natural and hydrometallurgical environments. Science of the Total Environment, 2022, 807, 150749.	3.9	2
107	PCBs and OCPs in sediments from Hongfeng Reservoir in Guizhou Province, China. Diqiu Huaxue, 2006, 25, 69-70.	0.5	1
108	Digestive solubilization of particle-associated arsenate by deposit-feeders: The roles of proteinaceous and surfactant materials. Environmental Pollution, 2019, 248, 980-988.	3.7	1

#	Article	IF	CITATIONS
109	Effect of pH on oxygen-induced abio-oxidation and removal of As from As-rich acid mine drainage in the co-existence of Zn(II). Applied Geochemistry, 2022, 140, 105298.	1.4	1
110	Must mercury enriched substrate be atmospheric mercury sources?. Diqiu Huaxue, 2006, 25, 27-27.	0.5	0
111	Distribution and speciation of mercury in surface water in Wanshan Hg-mined areas, Guizhou Province, China. Diqiu Huaxue, 2006, 25, 28-28.	0.5	0
112	Mercury emission from the indigenous mercury smelting in Wuchuan mercury mining areas, Guizhou Province, China. Diqiu Huaxue, 2006, 25, 235-235.	0.5	0
113	Different mercury species in the atmosphere over the municipal solid waste landfills. Diqiu Huaxue, 2006, 25, 238-238.	0.5	0
114	Total gaseous mercury emissions from mercury-enriched soil in Guizhou, China. Diqiu Huaxue, 2006, 25, 243-244.	0.5	0
115	Notice of Retraction: Comparison of Density Fractions of Heavy Metals (As, Cd, Cu and Pb) in Sediments Collected from Two Estuaries of Liaodong Gulf, China. , 2011, , .		Ο